



Fatty Acids Identified in the Burmese Python Promote Beneficial Cardiac Growth

Cecilia A. Riquelme, *et al.*

Science **334**, 528 (2011);

DOI: 10.1126/science.1210558

This copy is for your personal, non-commercial use only.

If you wish to distribute this article to others, you can order high-quality copies for your colleagues, clients, or customers by [clicking here](#).

Permission to republish or repurpose articles or portions of articles can be obtained by following the guidelines [here](#).

The following resources related to this article are available online at www.sciencemag.org (this information is current as of October 27, 2011):

Updated information and services, including high-resolution figures, can be found in the online version of this article at:

<http://www.sciencemag.org/content/334/6055/528.full.html>

Supporting Online Material can be found at:

<http://www.sciencemag.org/content/suppl/2011/10/27/334.6055.528.DC1.html>

<http://www.sciencemag.org/content/suppl/2011/10/27/334.6055.528.DC2.html>

This article **cites 25 articles**, 11 of which can be accessed free:

<http://www.sciencemag.org/content/334/6055/528.full.html#ref-list-1>

26. V. Joukov *et al.*, *Cell* **127**, 539 (2006).
 27. E. D. Coene *et al.*, *J. Cell Biol.* **192**, 497 (2011).
 28. M. E. Moynahan, J. W. Chiu, B. H. Koller, M. Jasini, *Mol. Cell* **4**, 511 (1999).

Acknowledgments: We thank X. Sun for technical assistance, V. Murty for advice, M. Wigler for discussions and encouragement, and NYSCF for access to the confocal microscope. This work was supported by NIH grants R01-CA137023 (R.B. and T.L.), P01-CA97403 (R.B. and T.L.), and R01-HD40916 (M.J.). R.S. was supported

by a Susan G. Komen Breast Cancer fellowship, L.J.R. by a Kirschstein National Research Service Award fellowship (F31-CA132626), C.R.R. by fellowships from the National Cancer Institute (T32-CA09503) and U.S. Department of Defense (DOD) (BC083089), and F.C. by a Kirschstein National Research Service Award fellowship (F32-HD51392). K.R. and J.B.H. were supported by grants to M. Wigler and J.B.H. from DOD (W81XWH04-1-0477) and the Breast Cancer Research Foundation. Microarray data have been deposited in the National Center for

Biotechnology Information's Gene Expression Omnibus (GEO) with GEO Series accession number GSE31673.

Supporting Online Material

www.sciencemag.org/cgi/content/full/334/6055/525/DC1
 Materials and Methods

Figs. S1 to S6
 References

16 June 2011; accepted 26 August 2011
 10.1126/science.1209909

Fatty Acids Identified in the Burmese Python Promote Beneficial Cardiac Growth

Cecilia A. Riquelme,¹ Jason A. Magida,¹ Brooke C. Harrison,¹ Christopher E. Wall,¹ Thomas G. Marr,² Stephen M. Secor,³ Leslie A. Leinwand^{1*}

Burmese pythons display a marked increase in heart mass after a large meal. We investigated the molecular mechanisms of this physiological heart growth with the goal of applying this knowledge to the mammalian heart. We found that heart growth in pythons is characterized by myocyte hypertrophy in the absence of cell proliferation and by activation of physiological signal transduction pathways. Despite high levels of circulating lipids, the postprandial python heart does not accumulate triglycerides or fatty acids. Instead, there is robust activation of pathways of fatty acid transport and oxidation combined with increased expression and activity of superoxide dismutase, a cardioprotective enzyme. We also identified a combination of fatty acids in python plasma that promotes physiological heart growth when injected into either pythons or mice.

The mammalian heart is a highly adaptable organ that demonstrates remarkable cellular remodeling in the face of both pathological and physiological stimuli. Pathological

hypertrophic signaling cascades, including those mediated by the $\alpha 1$ -adrenergic and endothelin receptors, can be activated by insults such as myocardial infarction, chronic hypertension, or genetic mutations affecting sarcomeric or calcium-handling proteins. This ultimately results in increased cell size, enhanced sarcomere assembly, and activation of a "fetal" gene program, with increased expression of β -myosin heavy chain (β -MHC), α -skeletal actin, atrial natriuretic peptide, and brain natriuretic peptide, accompanied by reduced expression of α -MHC and SERCA2 (sarco-

plasmic reticulum Ca^{2+} adenosine triphosphatase-2) (1–3).

Pathological insults also typically result in a switch in metabolic substrate utilization from lipid oxidation to glucose utilization and increased apoptosis and fibrosis (1, 3). Conversely, physiological cardiac hypertrophy resulting from postnatal growth, pregnancy, or exercise is primarily mediated by insulin-like growth factor-1 (IGF-1) signaling and activation of phosphatidylinositol 3-kinase (PI3K)–Akt signaling in the absence of fetal gene program activation (4, 5). Unlike pathological cardiac hypertrophy, this adaptive hypertrophy does not appear to be detrimental to cardiac function. In fact, exercise-induced physiological cardiac growth protects the heart against pathological stimuli such as pressure overload (6).

The infrequently feeding Burmese python (*Python molurus*) has been described as a model of extreme metabolic regulation in which many organs, including the heart, increase in mass after a large meal (7, 8). Whereas most mammalian models of physiological hypertrophy typically demonstrate modest hypertrophy (~10 to 20%) after weeks of stimulation, the python heart grows in mass by 40% within 48 to 72 hours after consumption of a large meal (7–9). This remarkable cardiac hypertrophy is accompanied by increased cardiac output and appears to be an adaptive response to support the large (factor of ~44) increase in postprandial metabolic rate, accompanied by increased systemic nutrient transport and widespread organ growth, required to accommodate such a large meal (7–12). The cardiac hypertrophy observed in *P. molurus* has

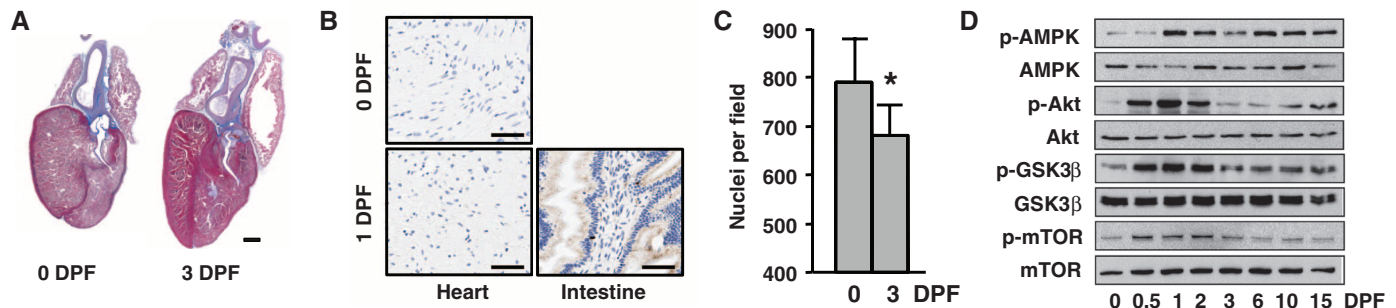


Fig. 1. Postprandial cardiac growth in the python is characterized by cellular hypertrophy and activation of protein synthesis pathways. **(A)** Masson trichrome-stained python hearts depicting pronounced postprandial cardiac hypertrophy. Scale bar, 2 mm. **(B)** BrdU staining of 0- and 1-dpf python hearts shows no evidence of postprandial cellular proliferation. Python small in-

testine is included as a positive control (brown nuclear staining). Scale bar, 50 μm . **(C)** The number of nuclei per field is reduced post-feeding. Error bars represent \pm SE; $n = 4$ per condition; * $P < 0.05$ versus 0 dpf. **(D)** Immunoblot analysis reveals increased phosphorylation of AMPK, Akt, GSK3 β , and mTOR in the postprandial python heart.

been described, but the underlying molecular and cellular mechanisms have yet to be determined (7, 8, 13). Given that pathological cardiac hypertrophy is a leading predictor of mortality, we sought to understand the cellular and molecular components of this rapid cardiac enlargement and potentially identify previously unknown mechanisms regulating physiological cardiac growth.

Similar to previous reports, we observed a progressive increase in heart size over the post-feeding time period (Fig. 1A and fig. S1A), with a maximum increase seen at 3 days post-feeding (dpf) (fig. S1A) (14). As in mammals, cardiac growth in the python appeared to be hypertrophic rather than hyperplastic, as there was no sign of 5-bromo-2'-deoxyuridine (BrdU) incorporation in the postprandial heart (Fig. 1B). Although the cellular architecture of the python ventricle did not allow for reliable quantification of myocyte size (fig. S1B), we observed a significant reduction in the number of nuclei per field in the 3-dpf ventricle, providing indirect evidence of cellular hypertrophy in the absence of cell division (Fig. 1C).

The fasted python myocardium was significantly more fibrotic than a normal mammalian

heart (~18% versus ~1 to 2%) (15), and the degree of fibrosis remained relatively unchanged throughout digestion of the meal (fig. S1C). The postprandial python heart demonstrated an atypical pattern of gene expression, with increased expression of both SERCA2 and α -skeletal actin mRNA, as well as a progressive increase in both *MYH7* (encoding β -MHC) and the less characterized striated muscle myosin heavy-chain gene *MYH15*, which also encodes the predominant MHC isoform expressed in the chicken heart (fig. S2) (16). Western blot analyses revealed increased phosphorylation of adenosine monophosphate-activated protein kinase (AMPK), Akt, glycogen synthase kinase-3 β (GSK3 β), and mammalian target of rapamycin (mTOR) during the postprandial period (Fig. 1D and fig. S3), indicating robust activation of protein synthetic pathways in the postprandial python heart.

Consistent with published observations (7), we observed a factor of 52 increase in plasma triglycerides (TAG) and a factor of 3 increase in non-esterified fatty acids (NEFAs) at 1 dpf (Fig. 2A). In most mammals, comparable plasma triglyceride concentrations would result in pathological lipid deposition in nonadipose tissues such

as the heart (17). In the python heart, however, thin-layer chromatography (TLC) and Oil Red O analysis did not reveal any evidence of lipid accumulation during the postprandial period (Fig. 2B and fig. S4A). We also found no change in cardiac transcript levels of very-low-density lipoprotein receptor, which suggests that utilization of triglyceride-rich lipoprotein particles is not altered after feeding (fig. S4B). Despite this lack of cardiac lipid accumulation, expression of the fatty acid transporter CD36 was increased by a factor of 13 at 1 dpf (Fig. 2C). mRNA levels of both muscle-type fatty acid binding protein (mFABP) and carnitine palmitoyltransferase 1B (CPT1B) were significantly increased after feeding (Fig. 2C), as were mitochondrial cytochrome oxidase (COX2) expression and nicotinamide adenine dinucleotide tetrazolium reductase (NADH-TR) staining (Fig. 2B). We also observed increased expression of several oxidative genes at 1 and 3 dpf, including medium-chain acyl-CoA dehydrogenase (MCAD), enoyl-CoA hydratase (ECHD), and acetyl-CoA acyltransferase 2 (ACAA2) (Fig. 2C). Together, these data suggest that there is increased oxidative capacity in the postprandial python heart.

These apparent alterations in mitochondrial electron transport chain flux were coupled with a significant increase in both expression and activity of the cardioprotective free radical-scavenging enzyme superoxide dismutase-2 (SOD2) (Fig. 2D) (18). We found no evidence of increased reactive oxygen species in the postprandial heart (fig. S5).

To investigate the possibility that the systemic changes observed in the python were due to circulating factors, we tested the effect of python plasma on neonatal rat ventricular myocytes (NRVMs) in culture. Treatment of NRVMs with fed plasma significantly increased cell size and α -actinin organization (Fig. 3A and fig. S6). The degree of NRVM growth induced by the specific postprandial plasma time points mimicked the time profile of in vivo python heart growth (Fig. 3A and fig. S1A), which suggests that the plasma concentrations of the hypertrophic factors varied throughout digestion. Whereas cells treated with the α -adrenergic agonist phenylephrine clearly showed robust activation of pathological patterns of gene expression, we found no such gene activation in cells treated with python plasma (Fig. 3B). We also determined that treatment of NRVMs with fed python plasma resulted in increased IGF-1 mRNA expression and enhanced the phosphorylation of mTOR and p70S6K (fig. S7). Intriguingly, fasted or fed python plasma significantly repressed activity of the transcription factor NFAT, a canonical indicator of pathological hypertrophic signaling, in NRVMs (Fig. 3C). Finally, treatment of NRVMs with fed python plasma significantly increased the expression of genes encoding key lipid-handling (mFABP) and metabolism proteins (CPT1B, MCAD, and ACAA2) in a manner similar to that observed in the fed python heart (fig. S8).

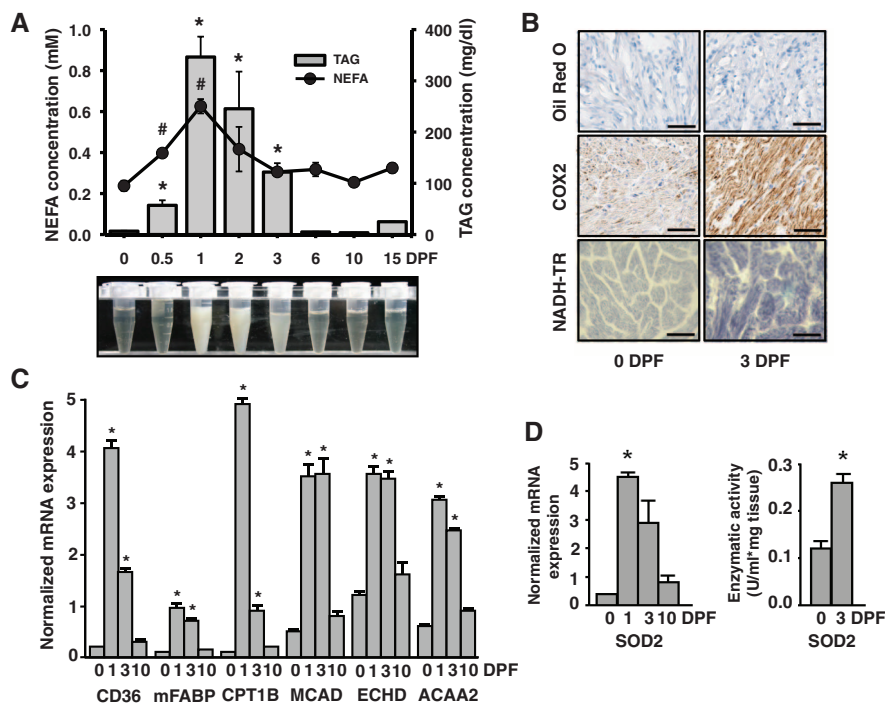


Fig. 2. The postprandial python heart has increased expression of fatty acid transport, handling, and oxidation genes along with enhanced free radical-scavenging capacity. **(A)** Plasma non-esterified fatty acid (NEFA) and triacylglyceride (TAG) concentrations are significantly increased after feeding. **(B)** Oil Red O staining reveals no cardiac accumulation of neutral lipids at 3 dpf. Mitochondrial staining is increased in the post-fed python heart as determined by cytochrome c oxidase II (COX2) immunostaining and NADH-tetrazolium reductase (NADH-TR) histochemistry. Scale bar, 50 μ m. **(C)** Increased mRNA expression of CD36, mFABP, CPT1B, and the β -oxidation proteins MCAD, ECHD, and ACAA2 is observed after feeding. **(D)** The mRNA expression and activity of mitochondrial SOD2 is increased post-feeding. Error bars represent \pm SE; $n = 4$ per condition; * $P < 0.05$ versus 0 dpf.

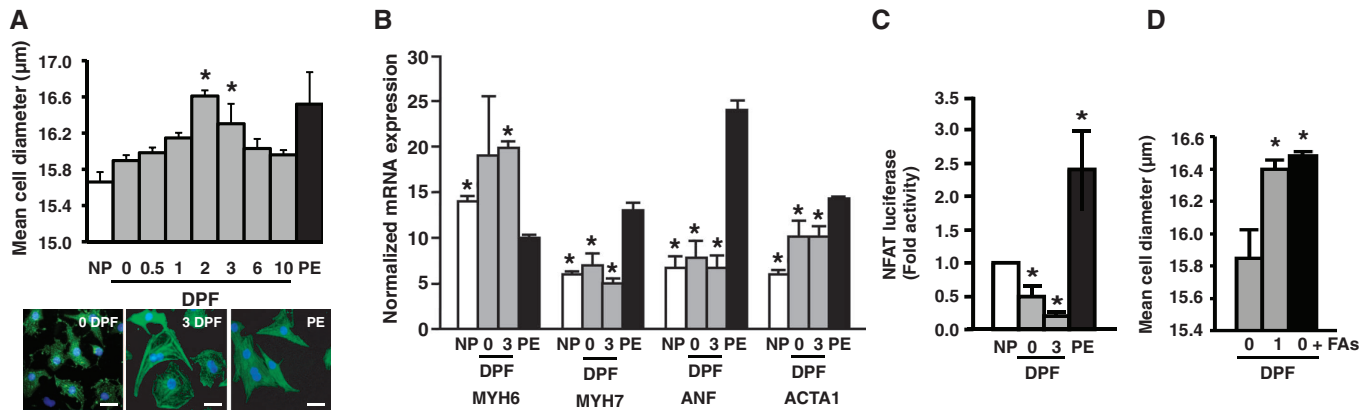


Fig. 3. Postprandial python plasma induces cardiomyocyte growth in vitro. **(A)** Fed python plasma induces cellular hypertrophy in neonatal rat cardiac myocytes (NRVMs). NP, no plasma; PE, phenylephrine (included as a positive control). The light microscope images show NRVMs stained for α -actinin (green) and nuclei (blue); scale bar, 10 μ m. **(B)** Python plasma does not induce the mRNA expression of known cardiac stress markers in NRVMs. ANF, atrial

natriuretic factor; MYH6, α -myosin heavy chain; MYH7, β -myosin heavy chain; ACTA1, α -skeletal actin. **(C)** Pathological NFAT signaling is repressed by python plasma. **(D)** Supplementing fasted python plasma with C14:0, C16:0, and C16:1 (0 dpf + FAs) results in cellular hypertrophy comparable to that seen with 1-dpf plasma. Error bars represent \pm SE; $n = 3$ per condition; * $P < 0.05$ versus 0 dpf [(A) and (D)]; * $P < 0.05$ versus PE (B); * $P < 0.05$ versus NP (C).

Given the substantial alterations seen in postprandial plasma lipid content and the evidence that heat treatment and protease K digestion were ineffective in eliminating the prohypertrophic effects of the fed python plasma (fig. S9), we focused our attention on lipid species as candidate prohypertrophic factors. We found that pretreatment of NRVMs with sulfosuccinimidyl oleate (SSO) (19), an irreversible inhibitor of CD36, completely blocked the prohypertrophic effect of fed plasma (fig. S10). We then analyzed fasted and post-fed python plasma by gas chromatography (GC) and observed a highly complex composition of circulating fatty acids with distinct patterns of abundance over the course of digestion (fig. S11). On the basis of these data, we identified five candidate fatty acids for further analysis (fig. S12) and determined that supplementing fasted python plasma with the 1-dpf molar ratio of C14:0 (myristic acid), C16:0 (palmitic acid), and C16:1 (palmitoleic acid) effectively recapitulated the increase in NRVM cell diameter seen with 1-dpf plasma (Fig. 3D). Similar to the effects seen with fed python plasma, treatment of NRVMs with this fatty acid mixture resulted in robust up-regulation of CD36, mFABP, CPT1, MCAD, and ACAA2 mRNA expression (fig. S8). Despite the established, pro-apoptotic properties of palmitic acid in cardiomyocytes (20–22), we did not find any evidence of apoptosis in NRVMs cultured in the presence of python plasma or the fatty acid combination (fig. S13). These data suggest that palmitoleic acid may protect cardiomyocytes from apoptosis in the presence of palmitic acid. Although the mechanism for this protection is unknown, it is possible that the presence of palmitoleic acid combined with increased oxidative capacity and free radical-scavenging capacity may act to reduce the generation of toxic, pro-apoptotic intermediates such as ceramide and reactive oxygen species, and to

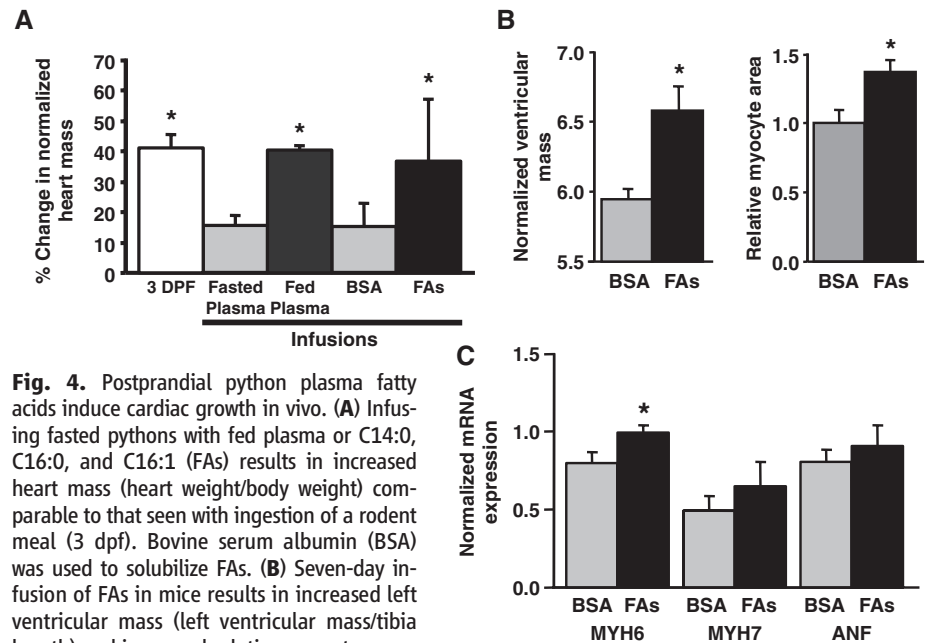


Fig. 4. Postprandial python plasma fatty acids induce cardiac growth in vivo. **(A)** Infusing fasted pythons with fed plasma or C14:0, C16:0, and C16:1 (FAs) results in increased heart mass (heart weight/body weight) comparable to that seen with ingestion of a rodent meal (3 dpf). Bovine serum albumin (BSA) was used to solubilize FAs. **(B)** Seven-day infusion of FAs in mice results in increased left ventricular mass (left ventricular mass/tibia length) and increased relative myocyte cross-sectional area. **(C)** FA infusion in mice results in a modest but statistically significant increase in MYH6 mRNA expression with no change in MYH7 or atrial natriuretic factor (ANF). Error bars represent \pm SE; $n = 3$ (A) or 6 [(B) and (C)] per condition; * $P < 0.05$ versus fasted python (A); * $P < 0.05$ versus BSA [(B) and (C)].

enhance the activity of cardioprotective pathways such as triglyceride biosynthesis and β -oxidation (21–23).

To investigate the ability of these fatty acids to trigger cardiac growth in vivo, we infused fasted pythons with the same mixture of myristic, palmitic, and palmitoleic acid and determined that this lipid infusion was as effective at stimulating cardiac growth as either feeding itself or infusion of plasma from a fed snake (Fig. 4A). We then administered the fatty acid mixture to

mice over a 7-day period and observed a significant increase in left ventricular mass (Fig. 4B), increased cardiomyocyte cross-sectional area (Fig. 4B), no activation of the pathological fetal gene program (Fig. 4C), and no evidence of alterations in cardiac fibrosis or lipid deposition (fig. S14). The growth-inducing effects of the fatty acids appeared to be cardiac-specific, as there were no observed alterations in either liver or skeletal muscle mass (fig. S15A). As a control, we also administered a mixture of oleic (C18:1),

linoleic (C18:2), and arachidonic (C20:4) acid in the molar ratio observed in the 1-dpf python and saw no evidence of cardiac hypertrophy (fig. S15B); this finding suggests that the prohypertrophic effects are specific to the mixture of myristic, palmitic, and palmitoleic acid. Palmitoleic acid was recently characterized as a lipokine that can modulate systemic insulin sensitivity (24). Additionally, fatty acid ethanolamides (FAEs) have been described as potent regulators of energy intake, and levels of the palmitoleic acid ethanolamide palmitoleylethanolamide (and other FAEs) are markedly increased in the fed python gastrointestinal tract (25). Together, these data and our data suggest multiple roles for palmitoleic acid and its metabolites in the regulation of insulin sensitivity, organ size, cardiac metabolism, and energy balance (24–26).

Our results indicate that postprandial cardiac growth in the python is characterized by cellular hypertrophy in the absence of hyperplasia and activation of physiological signaling pathways. Despite elevations in circulating triglycerides and increased fatty acid transport, the python heart appears to be protected from lipid deposition through increased oxidative capacity and induction of free radical-scavenging activity. Finally, we have shown that a combination of fatty acids, identified in postprandial python plasma, promotes physiological hypertrophy in mammalian cardiomyocytes. Given that activation of adaptive, physiological hypertrophic processes can provide functional benefit in the context of a cardiac

disease state, our data indicate that fatty acid supplementation may provide a new mechanism for modulating cardiac gene expression and function in mammals, and that such interventions could augment cardiac performance in the context of human disease.

References and Notes

- N. Frey, E. N. Olson, *Annu. Rev. Physiol.* **65**, 45 (2003).
- A. Calderone, N. Takahashi, N. J. Izzo Jr., C. M. Thaik, W. S. Colucci, *Circulation* **92**, 2385 (1995).
- E. N. Olson, *Nat. Med.* **10**, 467 (2004).
- B. C. Harrison *et al.*, *Mol. Cell. Biol.* **24**, 10636 (2004).
- R. Fagard, *Circulation* **103**, E28 (2001).
- J. P. Konhilas *et al.*, *Circ. Res.* **98**, 540 (2006).
- S. M. Secor, J. Diamond, *Nature* **395**, 659 (1998).
- J. B. Andersen, B. C. Rourke, V. J. Caiozzo, A. F. Bennett, J. W. Hicks, *Nature* **434**, 37 (2005).
- S. M. Secor, J. Diamond, *J. Exp. Biol.* **198**, 1313 (1995).
- S. M. Secor, J. Diamond, *Physiol. Zool.* **70**, 202 (1997).
- S. M. Secor, *J. Exp. Biol.* **211**, 3767 (2008).
- S. M. Secor, S. E. White, *J. Exp. Biol.* **213**, 78 (2010).
- C. E. Wall *et al.*, *Physiol. Genomics* **43**, 69 (2011).
- See supporting material on Science Online.
- A. Diwan *et al.*, *Circulation* **117**, 396 (2008).
- A. C. Rossi, C. Mammucari, C. Argentini, C. Reggiani, S. Schiaffino, *J. Physiol.* **588**, 353 (2010).
- R. S. Khan, K. Drosatos, I. J. Goldberg, *Curr. Opin. Clin. Nutr. Metab. Care* **13**, 145 (2010).
- T. Shimizu, H. Nojiri, S. Kawakami, S. Uchiyama, T. Shirasawa, *Geriatr. Gerontol. Int.* **10** (suppl. 1), 570 (2010).
- S. L. Coort *et al.*, *Mol. Cell. Biochem.* **239**, 213 (2002).
- G. C. Sparagna, D. L. Hickson-Bick, L. M. Buja, J. B. McMillin, *Antioxid. Redox Signal.* **3**, 71 (2001).
- T. A. Miller *et al.*, *Biochem. Biophys. Res. Commun.* **336**, 309 (2005).
- J. E. de Vries *et al.*, *J. Lipid Res.* **38**, 1384 (1997).
- D. L. Hickson-Bick, L. M. Buja, J. B. McMillin, *J. Mol. Cell. Cardiol.* **32**, 511 (2000).
- H. Cao *et al.*, *Cell* **134**, 933 (2008).
- G. Astarita *et al.*, *Am. J. Physiol. Regul. Integr. Comp. Physiol.* **290**, R1407 (2006).
- K. A. van der Lee *et al.*, *J. Lipid Res.* **41**, 41 (2000).

Acknowledgments: Supported by NIH grant HL050560 (L.A.L.), NSF grant IOS-0466139 (S.M.S.), University of Colorado Technology Transfer Office/State of Colorado grant OCG4999B (L.A.L. and T.G.M.), Hiberna Corporation (T.G.M. and S.M.S.), American Heart Association fellowship 0725732Z (C.A.R.), and NIH grant 5K01AR055676 (B.C.H.). L.A.L., T.G.M., and B.C.H. are on the scientific advisory board of, and are shareholders in, Hiberna Corporation, a company that is developing drugs based on natural models of extreme metabolic regulation. C.A.R. is a shareholder in Hiberna Corporation. The authors (L.A.L., C.A.R., J.A.M., B.C.H.) and the University of Colorado have filed a patent relating to methods and compositions for inducing physiological cardiac hypertrophy. We thank S. Cozza and T. Gleason for their technical assistance.

Supporting Online Material

www.sciencemag.org/cgi/content/full/334/6055/528/DC1
Materials and Methods
Figs. S1 to S15
Tables S1 to S3
References (27–32)

1 July 2011; accepted 15 September 2011
10.1126/science.1210558